



## Nano-FeS<sub>2</sub> for Commercial Li/FeS<sub>2</sub> Primary Batteries

Yang Shao-Horn,\* Steve Osmialowski and Quinn C. Horn\*<sup>z</sup>

Energizer, Incorporated, Westlake, Ohio 44145, USA

The rate capability of lithium cells containing a nano-FeS<sub>2</sub> pyrite sample was compared to that of micrometer-sized FeS<sub>2</sub> under an active material loading equivalent to that of commercial lithium battery electrodes. The nano-FeS<sub>2</sub> sample had an average particle size of 0.5 μm and each particle consisted of nano-FeS<sub>2</sub> crystals on the order of 50 nm. The rate capability of nano-FeS<sub>2</sub> was superior to that of the FeS<sub>2</sub> electrodes with an average crystal size of 10 μm but no improvement was found relative to the FeS<sub>2</sub> electrodes having an average crystal size of 1 μm. The rate capability of commercial Li/FeS<sub>2</sub> batteries may be limited by the ion conductivity of the electrolyte when FeS<sub>2</sub> samples have crystal sizes smaller than 1 μm.

© 2002 The Electrochemical Society. [DOI: 10.1149/1.1513558] All rights reserved.

Manuscript submitted March 6, 2002. revised manuscript received May 18, 2002. Available electronically October 9, 2002.

### Experimental

Commercial Li/FeS<sub>2</sub> AA primary batteries have offered substantially longer runtime than equivalent sized Zn/MnO<sub>2</sub> alkaline AA cells for high-power applications and below ambient temperature.<sup>1,2</sup> Recent research and development efforts in Li/FeS<sub>2</sub> batteries have been driven by remarkable performance improvements of alkaline batteries to meet ever-increasing power demands of electronic devices. It has been shown from our previous studies that the performance of the Li/FeS<sub>2</sub> system at high-current demands can be improved by reducing the crystal sizes of FeS<sub>2</sub> from 10 to 1 μm.<sup>3</sup> The effect of FeS<sub>2</sub> crystal sizes on the electrochemical performance of Li/FeS<sub>2</sub> cells is attributed to the fact that reduction in FeS<sub>2</sub> crystal size increases the presence of crystal boundaries or surfaces per unit volume of FeS<sub>2</sub>, provides a large number of nucleation sites for lithiated products, and thus promotes the kinetics of the heterogeneous (nonintercalation) lithiation process of FeS<sub>2</sub>.<sup>4</sup> Therefore, one may expect that nanocrystalline FeS<sub>2</sub> could further improve the rate capability of Li/FeS<sub>2</sub> cells at ambient temperature. In this study, we compare the electrochemical properties of nano-FeS<sub>2</sub> electrodes to those of micrometer-sized FeS<sub>2</sub> in lithium cells. Several recent studies have investigated the effect of nanocrystallinity on the electrochemical performance of lithium energy storage materials. Theoretically, the particle or crystal sizes of active materials can significantly modify the discharge capacities<sup>5</sup> and voltages<sup>6</sup> of intercalation electrodes, and the optimum particle or crystal sizes are dependent on electrode thickness.<sup>5</sup> Experimentally, nanocrystallinity of lithium intercalation compounds improves the rate capability of lithium rechargeable cells.<sup>7-9</sup> For nonintercalation electrodes such as intermetallic compounds<sup>10,11</sup> and some transition metal oxides,<sup>12</sup> nanocrystallinity enhances the reversibility of lithium reactions during electrochemical cycling. In these previous studies the advantage of nanocrystalline materials over conventional electrode materials has been demonstrated experimentally in very thin electrodes with low active material electrode loading (<10 mg/cm<sup>2</sup>). Commercial lithium battery electrodes are relatively thick, having considerably higher active material loading in the range of 14-25 mg/cm<sup>2</sup>. The effect of nanocrystalline active materials in thick electrode configurations on battery performance must be considered to use nanocrystalline materials in commercial lithium batteries. Here we examine the rate capability of nano-FeS<sub>2</sub> electrodes in relation to those of FeS<sub>2</sub> samples with micrometer-sized crystals in lithium cells under an active material loading equivalent to that of commercial lithium primary FeS<sub>2</sub> batteries (14-16 mg/cm<sup>2</sup>). The effect of nanocrystallinity on the discharge voltages and the lithiation mechanism of FeS<sub>2</sub> pyrite are discussed.

A nano-FeS<sub>2</sub> sample obtained from US Nanocorp, a natural (Chemetall) and a synthetic (Alfa AESAR) FeS<sub>2</sub> sample, having an average crystal size of 50 nm, 10 μm, and 1 μm, respectively,<sup>3</sup> were used in this study. The bulk chemical compositions of the FeS<sub>2</sub> samples were determined by inductively coupled plasma-atomic emission spectroscopy (ICP-AES) and the LECO method. The particle sizes and morphologies were examined using a cold emission scanning electron microscope (SEM) Hitachi S-4500 under the operating condition of 5 keV and 30° tilt. Structural analysis was performed by X-ray diffraction (XRD) on a Siemens D5000 diffractometer with Cu Kα radiation equipped with a graphite monochromator. The rate capability of nanocrystalline and micrometer-sized FeS<sub>2</sub> electrodes was determined by comparing the specific capacities in a 2016 coin cell package under current densities from 3 to 300 mA/g (0.042 to 4.2 mA/cm<sup>2</sup>) using an Arbin test system at 21 ± 2°C. Thin pellet-type FeS<sub>2</sub> electrodes were produced by compressing dry electrode mixes into expanded aluminum meshes. The FeS<sub>2</sub> electrode mix consisted of 49 wt % FeS<sub>2</sub>, 20 wt % graphite, 22 wt % acetylene black, 8 wt % ethylene/propylene copolymer, and 1 wt % polyethylene oxide (PEO). The average solid packing density was 50% and the average electrode loading of active materials was 14 mg/cm<sup>2</sup>. Two pieces of Celgard 2500 separator were used per cell. The electrolyte consisted of 1 M LiCF<sub>3</sub>SO<sub>3</sub> dissolved in 24.95 vol % dioxolane, 74.85 vol % dimethoxyethane, and 0.2 vol % dimethylisoxazole. A cell voltage cutoff of 0.9 V was used for all cells. Three duplicate cells were tested per current density and an average of specific capacities was obtained. Carbon contribution to the specific capacity of FeS<sub>2</sub> electrodes (up to a voltage cutoff of 0.9 V vs. lithium) was insignificant after examining the discharge capacities of coin cells containing carbon alone. The morphological features of “Li<sub>2</sub>FeS<sub>2</sub>” and “Li<sub>3.5</sub>FeS<sub>2</sub>” samples obtained from discharge of Li/nano-FeS<sub>2</sub> cells were examined in secondary electron imaging mode in the SEM. The Li<sub>x</sub>FeS<sub>2</sub> powder samples were dispersed on carbon tapes and exposed to air for a few seconds prior to loading into the microscope. No conductive coating was applied on the Li<sub>x</sub>FeS<sub>2</sub> particles.

### Results and Discussion

Chemical analysis showed that the nano-FeS<sub>2</sub> sample had a stoichiometric S/Fe ratio of 2. No other metal element had concentrations greater than 0.01% by weight. Therefore, it is expected theoretically that the discharge capacity of the nano-FeS<sub>2</sub> sample is 894 mAh/g by assuming reaction of 4 Li per FeS<sub>2</sub>. This value is similar to those of the natural and synthetic samples, 850 and 870 mAh/g, respectively, as reported previously.<sup>3</sup> XRD analysis revealed that nano-FeS<sub>2</sub> consisted primarily of the pyrite phase with space group *Pa*3,<sup>13</sup> with marcasite<sup>14</sup> as a minor impurity (marked by \*), as shown in Fig. 1a. Significant broadening in the X-ray powder dif-

\* Electrochemical Society Active Member.

<sup>z</sup> E-mail: horn@psicorp.com

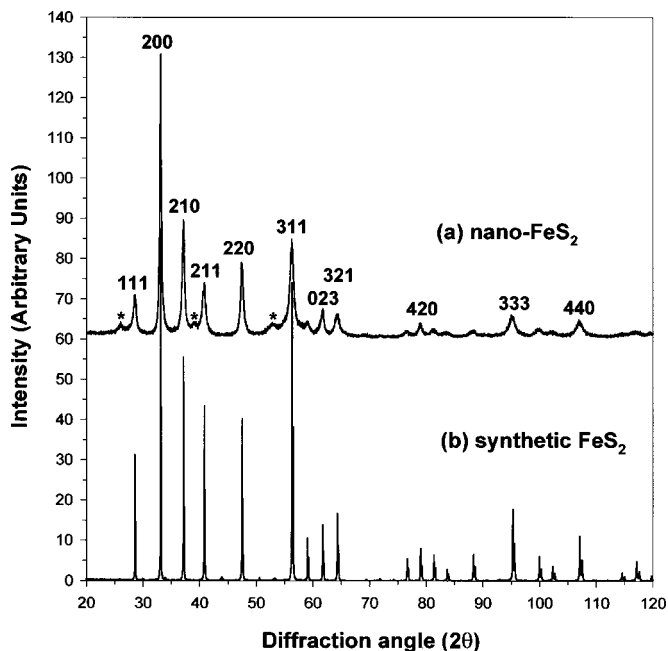


**Figure 1.** X-ray powder diffraction patterns of the (a) nano-FeS<sub>2</sub> and (b) synthetic FeS<sub>2</sub> samples with Cu K $\alpha$  radiation. The major pyrite diffraction peaks are indexed and the diffraction peaks of marcasite are marked by \* in (a).

fraction peaks was found for nano-FeS<sub>2</sub> with respect to the micrometer-sized samples. As the XRD patterns of natural and synthetic FeS<sub>2</sub> samples were nearly identical, only the synthetic FeS<sub>2</sub> pattern is shown in Fig. 1b for comparison. An average crystal size of nano-FeS<sub>2</sub> on the order of 50 nm was estimated from the  $\langle 200 \rangle$  XRD peak width according to the Scherrer equation.<sup>15</sup> This result was consistent with SEM studies of nano-FeS<sub>2</sub> powder. The nano-FeS<sub>2</sub> sample had an average particle size on the order of 0.5  $\mu\text{m}$ , and each particle contained nanocrystalline FeS<sub>2</sub> crystals in the range of 30 to 70 nm, as shown in Fig. 2.

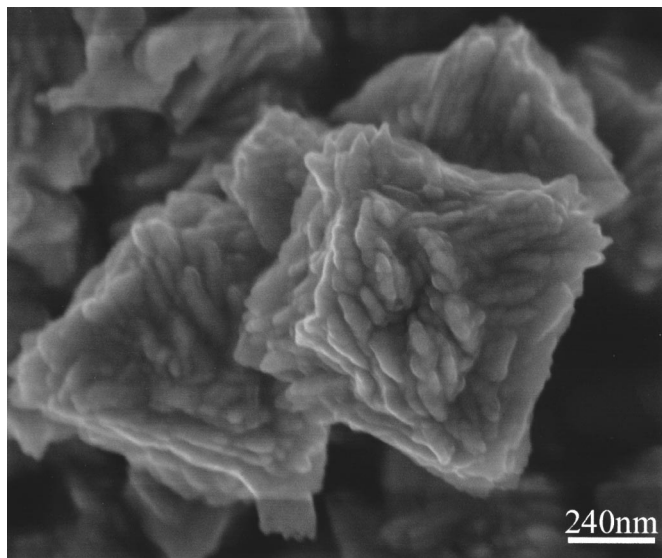


**Figure 2.** A typical secondary electron image of nano-FeS<sub>2</sub> powder. Each primary particle has an average size of 0.5  $\mu\text{m}$  and contains nanocrystals on the order of 50 nm.

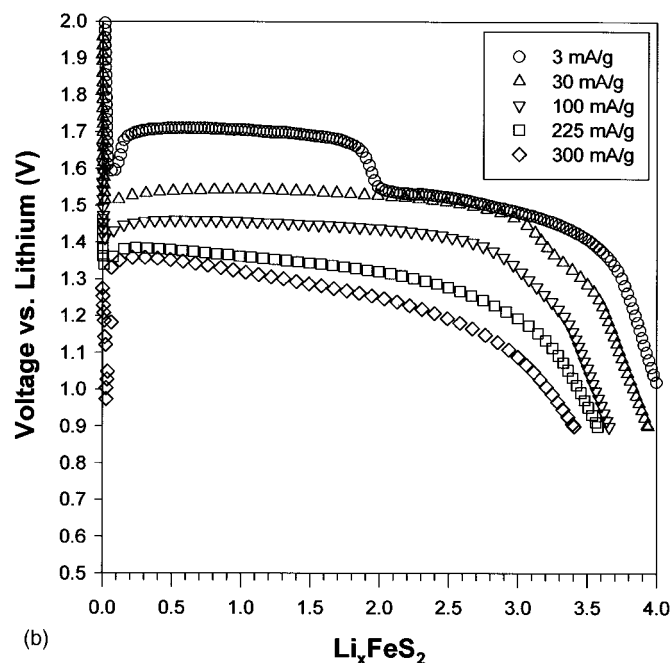
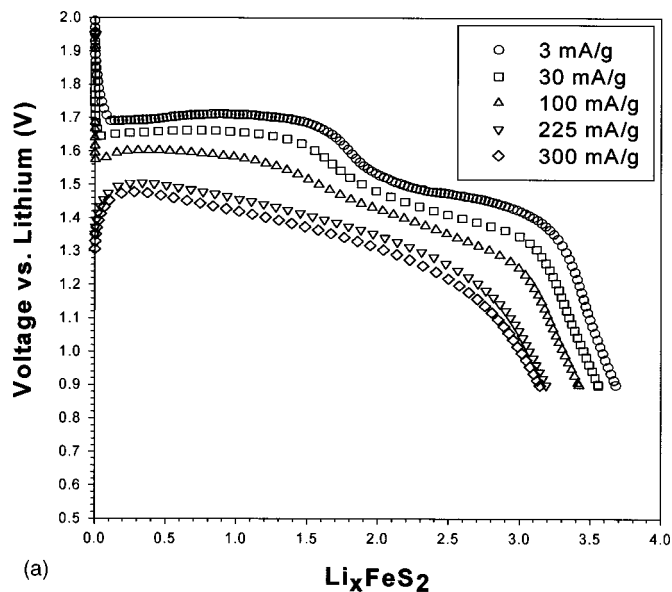
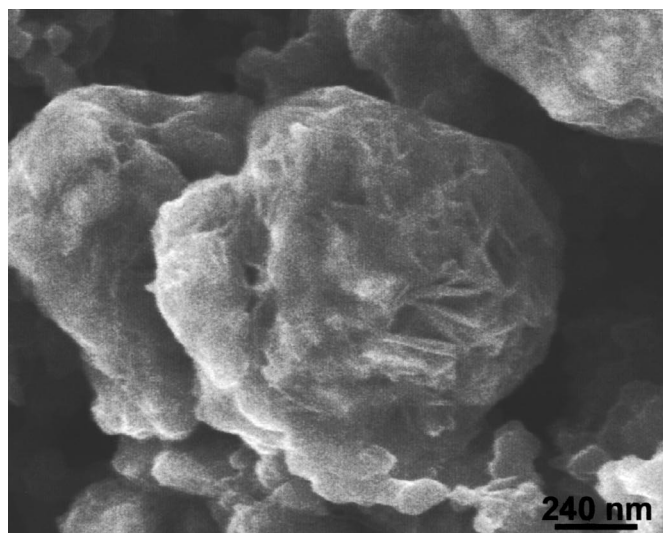
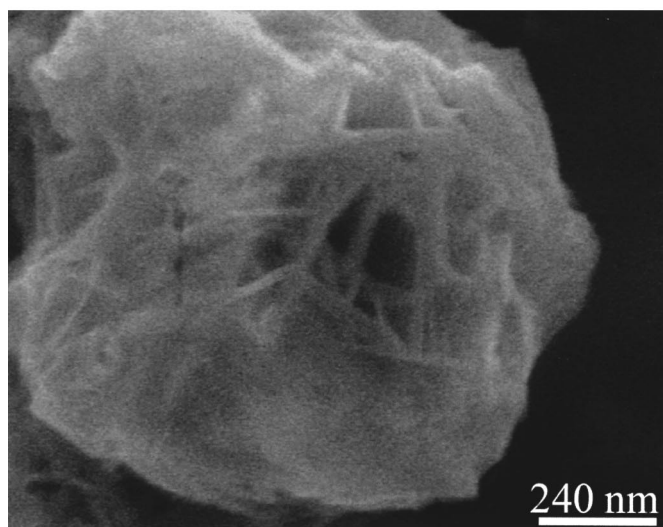


**Figure 3.** The voltage profiles of (a) Li/nano-FeS<sub>2</sub> and (b) Li/synthetic FeS<sub>2</sub> cells discharged under current densities of 3, 30, 100, 225, and 300 mA/g.

Discharge voltage profiles of Li/nano-FeS<sub>2</sub> cells were compared with those of synthetic FeS<sub>2</sub> in Fig. 3. A two-voltage-step reaction at 1.7 and 1.5 V was found for Li/nano-FeS<sub>2</sub> cells at current densities lower than 3 mA/g (0.042 mA/cm<sup>2</sup>) in Fig. 3a, which was similar to synthetic FeS<sub>2</sub> cells in Fig. 3b.<sup>3,4</sup> It is believed that the lithiation of nano-FeS<sub>2</sub> proceeds near equilibrium at these low current densities. Our previous studies of synthetic FeS<sub>2</sub><sup>4</sup> showed that the 1.7 V lithiation step was attributed to the formation of pyrrhotite Fe<sub>1-x</sub>S and Li<sub>2+x</sub>Fe<sub>1-x</sub>S<sub>2</sub> (0  $\leq$  x  $\leq$  0.33) intermediate phases, and the 1.5 V reaction produced a mixture of plate-shaped Li<sub>2</sub>S and amorphous Fe as final products. Although all the lithiated nano-FeS<sub>2</sub> electrodes at various lithium contents were comparable to those of synthetic FeS<sub>2</sub>.<sup>4</sup> Typical secondary electron images of lithiated FeS<sub>2</sub> particles with an average composition of Li<sub>2</sub>FeS<sub>2</sub> and Li<sub>3.5</sub>FeS<sub>2</sub> are



(a)



(b)

**Figure 4.** Typical secondary electron images of lithiated FeS<sub>2</sub> particles with an average composition of (a) Li<sub>2</sub>FeS<sub>2</sub> and (b) Li<sub>3.5</sub>FeS<sub>2</sub>.

shown in Fig. 4a and b, respectively. Plate-like crystals, presumably Li<sub>2</sub>S, were found on the surface of the Li<sub>2</sub>FeS<sub>2</sub> particles in Fig. 4a, and throughout the Li<sub>3.5</sub>FeS<sub>2</sub> particles in Fig. 4b. In contrast to extensive cracking observed in lithiated micrometer-sized natural and synthetic FeS<sub>2</sub> particles,<sup>4</sup> the nano-FeS<sub>2</sub> particle morphology was retained upon lithiation despite considerable particle expansion and the formation of plate-like Li<sub>2</sub>S (the most evident in Fig. 4b). The Li<sub>2</sub>S plates had a thickness on the order of 20 nm, similar to those formed upon final lithiation of synthetic FeS<sub>2</sub>.<sup>4</sup> It is believed that the two-voltage-step lithiation of nano-FeS<sub>2</sub> follows a similar reaction mechanism to that of synthetic FeS<sub>2</sub>.<sup>4</sup> In addition, the sharp 1.7 to 1.5 V transition in the voltage profiles of micrometer-sized FeS<sub>2</sub> cells was considerably rounded in Li/nano-FeS<sub>2</sub> cells, which could be attributed to the nanocrystalline sizes of FeS<sub>2</sub>. Similar rounding effects were previously modeled and proposed by Obrovac and Dahn for nanocrystalline lithium intercalation materials in quasi equilibrium.<sup>6</sup>

Upon increasing current densities from 3 mA/g (0.042 mA/cm<sup>2</sup>) to 300 mA/g (4.2 mA/cm<sup>2</sup>), lithiation of FeS<sub>2</sub> at 1.7 V was slowly

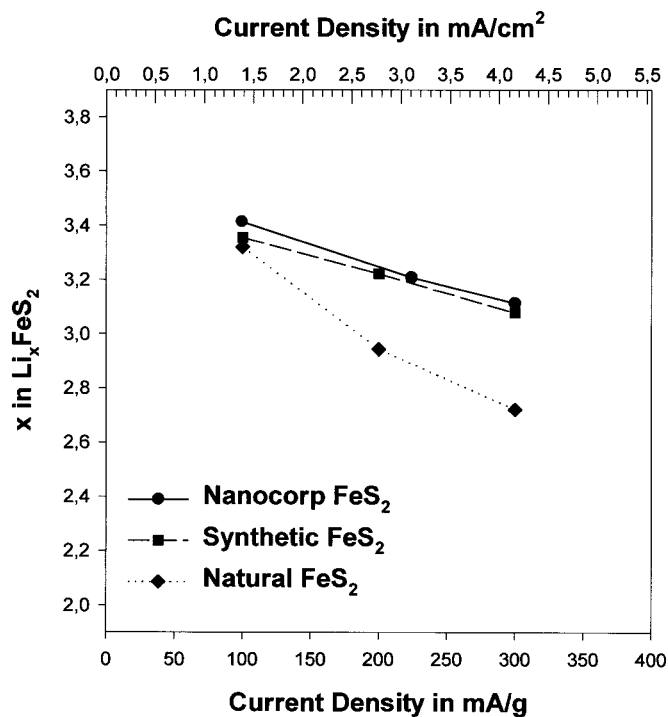


**Figure 5.** The average lithium contents in the discharged FeS<sub>2</sub> electrodes as a function of current density in mA/g and mA/cm<sup>2</sup>.

suppressed in nano-FeS<sub>2</sub> electrodes as the two-voltage-step reaction of nano-FeS<sub>2</sub> electrodes gradually changed to a sloping voltage process. This was in contrast to the sharp transition from the two-voltage-step (at 1.7 and 1.5 V) to the one-voltage-step (at 1.5 V) observed for micrometer-sized FeS<sub>2</sub> electrodes, as shown in Fig. 3b.<sup>3,4</sup> The stability of the 1.7 V lithiation step in nano-FeS<sub>2</sub> electrodes between 3 mA/g (0.042 mA/cm<sup>2</sup>) and 100 mA/g (1.4 mA/cm<sup>2</sup>) could be attributed to nanocrystalline sizes of FeS<sub>2</sub>, which provided sufficient nucleation sites for the formation of intermediate phases upon lithiation of FeS<sub>2</sub>. Specific discharge capacities of nano-FeS<sub>2</sub> electrodes were compared with those of micrometer-sized electrodes in lithium cells as a function of current density in mA/g and mA/cm<sup>2</sup>, as shown in Fig. 5. Nano-FeS<sub>2</sub> and synthetic FeS<sub>2</sub> electrodes were superior to natural FeS<sub>2</sub> electrodes at current densities greater than 100 mA/g. However, no improvement in the rate capability of Li/nano-FeS<sub>2</sub> (50 nm crystallites) cells was found with respect to that of lithium synthetic FeS<sub>2</sub> (1 μm crystallites) cells. This observation can be explained by the following hypothesis that at high current densities the ionic conductivity of the electrolyte, rather than the FeS<sub>2</sub> crystal sizes, limits the lithiation process of FeS<sub>2</sub> particles when the average size of FeS<sub>2</sub> crystals are less than 1 μm and the as-described electrode configuration is used. Reduced electrode loading or thickness can decrease the concentration polarization in the electrode induced by the limiting ionic conductivity of electrolyte during discharge. Therefore, the FeS<sub>2</sub> crystal size eventually limits the kinetics of Li/FeS<sub>2</sub> cells if the electrode loading of FeS<sub>2</sub> in g/cm<sup>2</sup> is reduced sufficiently. Although nanomaterials could effectively improve the rate capability of lithium cells that contain thin electrodes,<sup>7-9</sup> the advantage of nanocrystalline materials may not be realized in commercial lithium battery electrodes with high active material loading, particularly at the 25 mg/cm<sup>2</sup> level. The limiting material parameter on the high-rate performance of lithium batteries strongly depends on the lithium reaction mechanisms, the electrode configuration, and the electrolyte ionic conductivity. Therefore, application of nanocrystalline electrochemically active materials in lithium battery electrodes alone does not neces-

sarily lead to improvement in the rate capability of commercial lithium batteries.

### Conclusions

Two-voltage-step lithiation of nano-FeS<sub>2</sub> (Nanocorp, 50 nm) proceeded similarly to that of synthetic FeS<sub>2</sub> reported previously.<sup>4</sup> Using an electrode loading equivalent to those of commercial lithium battery electrodes, the performance of nano-FeS<sub>2</sub> electrodes was superior to that of FeS<sub>2</sub> electrodes with an average crystal size of 10 μm, but equivalent to the FeS<sub>2</sub> electrodes having an average crystal size of 1 μm. It is believed that the ionic conductivity of the electrolyte, rather than FeS<sub>2</sub> crystal sizes, limited the commercial Li/FeS<sub>2</sub> battery performance when the FeS<sub>2</sub> had an average crystal size smaller than 1 μm.

### Acknowledgments

Permission from Energizer to publish this work is greatly acknowledged. The authors thank Weiwei Huang, Richard Middaugh, and Jack Marple from Energizer for fruitful discussions.

*Energizer Battery Company assisted in meeting the publication costs of this article.*

### References

1. Hi Energy Lithium Application Manual, Energizer Power Systems, Westlake, OH (1993).
2. *Lithium-Iron Disulfide Cells*, M. B. Clark, Editor, Academic Press, New York (1982).
3. Y. Shao-Horn and Q. C. Horn, *Electrochim. Acta*, **46**, 2613 (2001).
4. Y. Shao-Horn, S. Osmialowski, and Q. C. Horn, *J. Electrochem. Soc.*, In press.
5. G. S. Nagarajan, J. W. Van Zee, and R. M. Spotnitz, *J. Electrochem. Soc.*, **145**, 771 (1998).
6. M. N. Obrovac and J. R. Dahn, *Phys. Rev. B*, **61**, 6713 (2000).
7. J. Kim and A. Manthiram, *J. Electrochem. Soc.*, **146**, 4371 (1999).
8. N. Li, J. Patrissi, G. Che, and C. R. Martin, *J. Electrochem. Soc.*, **147**, 2044 (2000).
9. S.-H. Kang, J. B. Goodenough, and L. K. Rabenberg, *Electrochem. Solid-State Lett.*, **4**, A49 (2001).
10. O. Mao, R. L. Turner, I. A. Courtney, B. D. Frederickson, M. I. Buckett, L. J. Krause, and J. R. Dahn, *Electrochem. Solid-State Lett.*, **2**, 3 (1999).
11. O. Mao, R. A. Dunlap, and J. R. Dahn, *Solid State Ionics*, **118**, 99 (1999).
12. P. Poizot, S. Laruelle, S. Grugeon, L. Dupont, and J. M. Tarascon, *Nature (London), Phys. Sci.*, **407**, 496 (2000).
13. Joint Commission of Powder Diffraction File Set no. 42-1340.
14. Joint Commission of Powder Diffraction File Set no. 37-0475.
15. B. D. Cullity, *Elements of X-Ray Diffraction*, Addison-Wesley Publishing Co., Reading, MA (1978).